The Effect of Gibbs Adsorption on Marangoni Instability in Penetration Mass Transfer

P. L. T. BRIAN and J. R. ROSS

Department of Chemical Engineering
Massachusetts Institute of Technology
Cambridge, Massachusetts 02139

A theoretical analysis of Marangoni convection in gas-liquid mass transfer shows the stabilizing effect of surface convection in the Gibbs adsorption layer. Results are obtained for various ratios of liquid layer thickness to mass transfer penetration depth. For deep liquid layers, complete stabilization results when the inventory in the Gibbs layer equals the solute deficiency in the liquid phase boundary layer, irrespective of the shape of the unperturbed concentration profile.

This new theory agrees much better with experimental results than did previous theories. For example, for triethylamine desorption from water, the discrepancy is reduced from a factor of 8,000 to a factor of 8. Speculations are offered concerning this residual discrepancy.

SCOPE

Interphase mass transfer is often accompanied by cellular convection at the interface, induced by surface tension gradients which result from solute concentration gradients or temperature gradients. Called Marangoni instability, the convection may become so intense in liquid-liquid extraction systems that it causes spontaneous emulsification. Even in gas-liquid systems, Marangoni convection has been known to enhance the mass transfer rate more than ten-fold. Furthermore, the cellular convection can lead to serious quality control problems when it occurs in the drying of paint films and in other surface coating processes.

Previous theoretical work on the problem has consisted of hydrodynamic stability analyses to predict the point of convective instability, as measured by the critical value of the Marangoni number. Recent measurements (Brian et al., 1971) of the critical Marangoni number in desorbing surface tension-lowering solutes from water were found to lie two to four orders of magnitude above previously published theoretical predictions, and one speculation offered to explain the discrepancy involved the Gibbs adsorption of the transferring solute. A solute which depresses the surface tension must, according to the Gibbs theory (Adamson, 1967), adsorb at the surface, and the effect of this adsorption had not been considered in previous theoretical studies.

A small disturbance hydrodynamic stability analysis (Brian, 1971) then revealed that surface convection of solute in the Gibbs layer has a profound stabilizing effect on Marangoni convection. Measured by an adsorption number $\mathcal{A}$, surface convection completely stabilizes the system, raising the critical Marangoni number to infinity when $\mathcal{A}$ exceeds a critical value. This analysis demonstrated the importance of surface convection in the Gibbs layer, but due to simplifications invoked it could not be applied quantitatively to the experimental results. The theory assumed a linear concentration gradient throughout the liquid layer, while the experiments involved penetration mass transfer with a liquid layer thickness substantially greater than the mass transfer penetration depth.

The present analysis incorporates the effect of Gibbs adsorption into a theoretical model of Marangoni instability which involves penetration-type mass transfer such as that encountered in the experiments. The model is an extension of that employed by Vidal and Acrivos (1968), who did not consider the effect of Gibbs adsorption. The present results show the effects of Gibbs adsorption on the critical Marangoni number at various values of λ, the ratio of the liquid depth to the mass transfer penetration depth.

CONCLUSIONS AND SIGNIFICANCE

General definitions are proposed for the Marangoni number M and the adsorption number $\mathcal{A}$. The critical value of $\mathcal{A}$, at which surface convection in the Gibbs layer completely stabilizes the system, is found to increase with increasing liquid depth. For very deep liquid layers this critical value approaches 0.5, irrespective of the shape of the unperturbed concentration profile in the liquid phase and irrespective of $\mathcal{R}$, the liquid-to-gas phase resistance ratio. At this point the quantity of solute in the Gibbs adsorpion layer just equals the solute deficiency in the liquid phase concentration boundary layer.

It is further shown that the product $\mathcal{A}M$, which involves only the solute properties and not the mass transfer driving force, is a useful measure of the importance of Gibbs ad-

sorption. For gas phase-controlled mass transfer, for example, when $\mathcal{M} << 2$, Gibbs adsorption has a negligible influence; when $\mathcal{M} >> 2$, Gibbs adsorption dominates, and the critical adsorption number is more significant than the critical Marangoni number.

In applying these results to penetration-type mass transfer, solute storage in the Gibbs layer may have an important effect on the rate of transfer from the liquid phase before Marangoni instability occurs. Therefore, the inventory in the Gibbs layer at the start of the contact interval becomes a significant parameter which is difficult to evaluate in experimental situations.

Nevertheless this new theory shows much better agreement with the experimental results than did previous theories. For example, for triethylamine desorption from water, the discrepancy is reduced from a factor of 8,000 to a factor of 8. Some speculations are offered concerning this residual discrepancy.

THEORETICAL MODEL

In the unperturbed state, a solute is diffusing from a horizontal stagnant liquid layer into a gas phase above. The solute depresses the surface tension of the liquid, and this may result in Marangoni instability, but buoyancy effects and thermal effects on desorption are assumed to be negligible. The solute concentration in the liquid phase is equal to C_i at the liquid surface and increases with depth into the liquid phase, asymptotically approaching the value C_B in the bulk liquid, as shown in Figure 1a. The depth of the liquid layer is l, but C varies only within a relatively thin concentration boundary layer near the surface, characterized by the boundary layer thickness h, to be defined quantitatively later on.

In a penetration theory model of gas-liquid mass transfer this concentration profile would be transient, with the boundary layer thickness increasing with time. Following earlier workers who studied buoyancy-induced convective instability, Vidal and Acrivos (1968) employed a "frozen profile" analysis of Marangoni convection in which the time rate of change of the unperturbed profile is neglected. They then performed a stability analysis on the frozen profile to determine if a perturbation would grow or decay.

In the context of buoyancy-driven convective instability, a number of investigators have assessed the adequacy of the frozen-profile analysis. It appears (Mahler et al., 1968) that the frozen-profile analysis does give a reasonably accurate prediction of the point at which a perturbation just begins to grow, but the initial growth rate is slow, and considerable time elapses before the perturbation has grown by a substantial amount and is then growing at a fast rate. Thus experimental measurements (Spangenberg and Rowland, 1961; Foster, 1965b; Blair and Quinn, 1969) reveal the onset of measurable convection at substantially longer times than predicted by the frozen-profile analysis. This has led several investigators to perform a transient analysis of the problem, in which the rate of change of the unperturbed profile with time is considered. These results have shown better agreement with the experiments, but their interpretation is beclouded by the necessity of making subjective judgements regarding the nature of the initial perturbations and the amount of growth required before the convection is experimentally visible (compare Foster, 1965a and 1968; Mahler et al., 1968; Gresho and Sani, 1971).

Since the focus of the present work is upon the effect of Gibbs adsorption, it seems appropriate to employ the frozen-profile simplification, at least initially. Comparison of the present results with those of Vidal and Acrivos (1968) will then reveal the effect of Gibbs adsorption without the complications inherent in the complete transient analysis.

Another compulsion to adopt the frozen-profile simplification in this study stems from a desire to apply the results to steady state experiments in a wetted-wall column, such as those of Brian et al. (1971). In these experiments the unperturbed concentration profile is steady in time but is developing in downstream *distance*, or contact time. In this context, the frozen-profile assumption corresponds to neglecting the rate of change of the unperturbed concentration profile with downstream distance. For this system, it can be shown by inspection of the linearized differential equations that the unperturbed velocity profile has no effect on that disturbance mode which is invariant with downstream distance, that is, for stationary roll cells with axes aligned in the flow direction. By analogy to buoyancy-driven instability (compare Gallagher and Mercer, 1965; Deardorff, 1965), this is expected to be the least stable mode in the presence of the mean flow, and thus the critical Marangoni number is unaltered by the flow. Furthermore, this disturbance mode cannot propagate downstream, and thus the time required for such a disturbance to grow to a visible magnitude is of no consequence, and the convection will be observed if the point of inception of instability is reached within the wetted-wall column. In this context it is expected, therefore, that the frozen-profile analysis will be more suitable than a complete analysis of a transient penetration problem.

The present analysis will consequently be based on the frozen-profile assumption that the unperturbed concentration profile is steady in time and is invariant with position in the plane of the liquid surface.

The fluid mechanics of the gas phase are not considered, the transfer of solute from the gas-liquid interface to the bulk gas phase being modeled by a gas phase mass transfer coefficient k_G assumed to be constant and independent of convection within the liquid phase. Also, deformation of the gas-liquid interface from its initial planar state is neglected, as are surface viscosity and elasticity effects. These simplifications are believed to be acceptable for gas-liquid systems in which high polymers are not present (compare Pearson, 1958; Scriven and Sternling, 1964; Smith, 1966; Brian et al., 1971).

The infinitesimal perturbations in the z-direction velocity and in the solute concentration are assumed to be of the form

$$w = (\mathcal{D}/h)\, F(\xi, \zeta)\, f(\eta)\, e^{p\tau} \tag{1}$$

$$c = (C_B - C_i)\, F(\xi, \zeta)\, g(\eta)\, e^{p\tau} \tag{2}$$

The function $F(\xi, \zeta)$ describes a periodic variation in the x and y directions, which lie in the plane of the gas-liquid interface. The function is defined by the differential equation

$$\frac{\partial^2 F}{\partial \xi^2} + \frac{\partial^2 F}{\partial \zeta^2} + \alpha^2 F = 0 \tag{3}$$

in which α is the dimensionless wave number for the periodic variation. Inserting Equations (1), (2), and (3) into the linearized equations of motion and the diffusion-convection equation for transport of the solute yields

(compare Pearson, 1958) the differential equations defining f and g

$$[p - Sc(D^2 - \alpha^2)](D^2 - \alpha^2) f = 0 \quad (4)$$

$$[(D^2 - \alpha^2) - p]g = \Phi' f \quad (5)$$

where D represents differentiation with respect to the dimensionless depth coordinate η. The unperturbed concentration profile is expressed in dimensionless form as

$$\frac{C - C_i}{C_B - C_i} = \Phi(\eta) \quad (6)$$

and Φ' represents the derivative of Φ with respect to η.

At a dimensionless depth λ, corresponding to the bottom wall, the no-slip velocity condition requires that

$$f(\lambda) = 0 \quad (7)$$

$$f'(\lambda) = 0 \quad (8)$$

The concentration boundary condition at the bottom wall will correspond either to a constant concentration at a conducting wall

$$g(\lambda) = 0 \quad (9a)$$

or to a constant solute flux at an insulating wall

$$g'(\lambda) = 0 \quad (9b)$$

as discussed by Pearson (1958) and Brian (1971).

The normal velocity must vanish at the nondeformable gas-liquid interface:

$$f(0) = 0 \quad (10)$$

The tangential shear stress condition at the free surface introduces the Marangoni number into the problem

$$f''(0) = M \alpha^2 g(0) \quad (11)$$

It should be noted that the Marangoni number is defined here in terms of the overall concentration difference in the liquid phase and h the thickness of the liquid phase concentration boudary layer.

The effect of Gibbs adsorption enters the problem through the concentration boundary condition at the free surface

$$g'(0) = \Re g(0) + p\mathcal{G} g(0) + \alpha^2 \mathcal{S} g(0) - \mathcal{R} f'(0) \quad (12)$$

It is assumed that the quantity of solute adsorbed at the surface Γ is related to the concentration at the surface C_i by the Gibbs adsorption isotherm $\Gamma = \sigma C_i/RT$. The derivation of Equation (12) and a discussion of its significance are given by Brian (1971). The term on the left-hand side of Equation (12) represents diffusion of solute to the surface from the liquid beneath. The terms on the right-hand side represent transfer to the gas phase, accumulation within the Gibbs layer, surface diffusion within the Gibbs layer, and surface convection within the Gibbs layer, respectively.

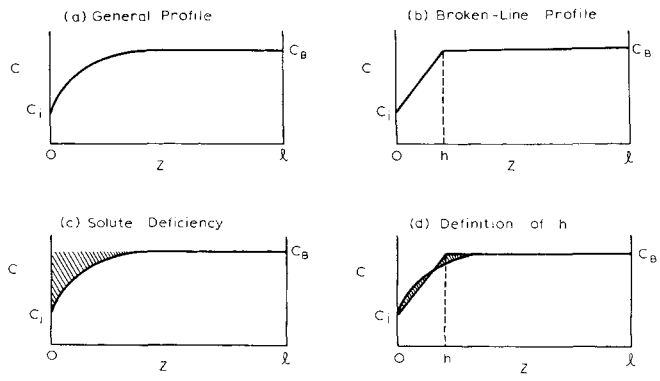

Fig. 1. Unperturbed concentration profile.

In seeking solutions for the case of neutral stability in which an infinitesimal perturbation neither grows nor decays, p will be taken to be zero. This corresponds to the assumption that no oscillatory modes of instability exist, an assumption which has been justified by Brian and Smith (1972) for the case in which a linear concentration gradient extends throughout the liquid layer. With $p = 0$, $\mathcal{G}$ drops out of Equation (12), and accumulation within the Gibbs layer has no influence on the neutrally stable state.

The statement of the problem is now complete, and a solution can be obtained for a specified function $\Phi(\eta)$, representing the shape of the unperturbed concentration profile.

SOLUTION FOR FINITE LIQUID DEPTH

When the value of λ is finite, it is useful to simplify the problem by considering only the case of a broken line unperturbed concentration profile, as shown in Figure 1b where the definition of h is apparent. The normalized slope of the unperturbed concentration profile is given by

$$\Phi' = \begin{Bmatrix} 1 \text{ for } 0 \leq \eta < 1 \\ 0 \text{ for } 1 < \eta \leq \lambda \end{Bmatrix} \quad (13)$$

With p taken to be zero, the solution to Equation (4) subject to the condition of Equation (10) may be written

$$f = A_1 \sinh \alpha\eta + A_2 \eta \sinh \alpha\eta + A_3 \eta \cosh \alpha\eta \quad (14)$$

Employing Equations (7) and (8) yields

$$\frac{A_3}{A_1} = -\frac{(\sinh \alpha\lambda)^2}{\alpha\lambda^2} \quad (15)$$

$$\frac{A_2}{A_1} = \frac{(\sinh \alpha\lambda)(\cosh \alpha\lambda)}{\alpha\lambda^2} - \frac{1}{\lambda} \quad (16)$$

The concentration function is written in the form

$$g(\eta) = \begin{Bmatrix} g_1(\eta) \text{ for } 0 \leq \eta < 1 \\ g_2(\eta) \text{ for } 1 < \eta \leq \lambda \end{Bmatrix} \quad (17)$$

Employing Equation (13) and taking $p = 0$, the solution to Equation (5) is

$$g_1(\eta) = B_1 \sinh \alpha\eta + B_2 \cosh \alpha\eta + \Psi(\eta) \quad (18)$$

$$g_2(\eta) = B_3 \sinh \alpha\eta + B_4 \cosh \alpha\eta \quad (19)$$

where the function Ψ is defined as

$$\Psi(\eta) \equiv -\left[\frac{A_2}{4\alpha^2}\right] \eta \sinh \alpha\eta + \left[\frac{A_1}{2\alpha} - \frac{A_3}{4\alpha^2}\right] \eta \cosh \alpha\eta + \left[\frac{A_3}{4\alpha}\right] \eta^2 \sinh \alpha\eta + \left[\frac{A_2}{4\alpha}\right] \eta^2 \cosh \alpha\eta \quad (20)$$

The constants in Equations (18) and (19) are determined from the previously stated boundary conditions plus two additional conditions requiring the continuity of the function g and its first derivative at $\eta = 1$:

$$g_1(1) = g_2(1) \quad (21)$$

$$g_1'(1) = g_2'(1) \quad (22)$$

Employing Equations (12), (21), (22), and (9a) or (9b), the constants are determined as

$$B_1 = \frac{(\mathcal{R} + \alpha^2\mathcal{S})[\alpha G\Psi(1) - \Psi'(1)] - \alpha(\sinh\alpha - G\cosh\alpha)[\Psi'(0) + \mathcal{A}(\alpha A_1 + A_3)]}{\alpha(\mathcal{R} + \alpha^2\mathcal{S})(\cosh\alpha - G\sinh\alpha) + \alpha^2(\sinh\alpha - G\cosh\alpha)} \tag{23}$$

$$B_2 = \frac{\alpha G\Psi(1) - \Psi'(1) - B_1\alpha(\cosh\alpha - G\sinh\alpha)}{\alpha(\sinh\alpha - G\cosh\alpha)} \tag{24}$$

$$B_3 = \frac{B_1\sinh\alpha + B_2\cosh\alpha + \Psi(1)}{\sinh\alpha - \left(\frac{\sinh\alpha\lambda}{\cosh\alpha\lambda}\right)^{\nu}\cosh\alpha} \tag{25}$$

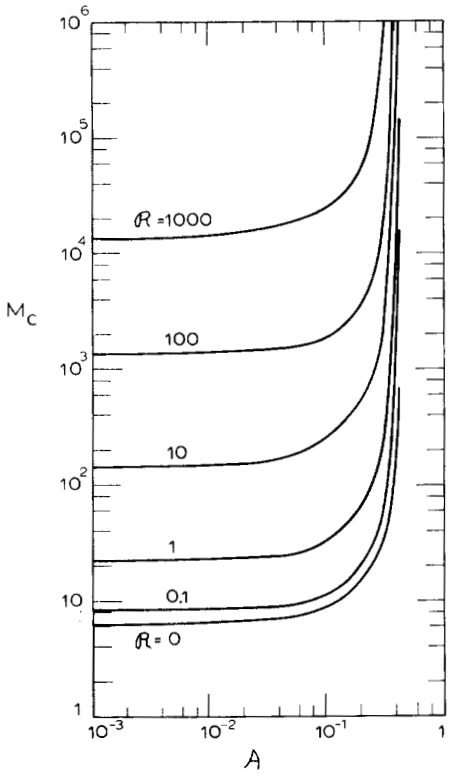

Fig. 2. Effect of $\mathcal{A}$ on M_c for insulating case, $\lambda = 10$, $\mathcal{S} = 0$.

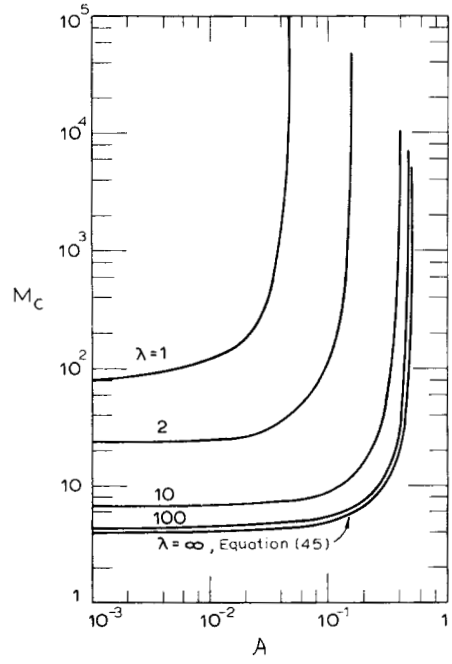

Fig. 3. Effect of liquid depth on M_c for insulating case, $\mathcal{R} = 0$, $\mathcal{S} = 0$.

$$B_4 = -\left(\frac{\sinh\alpha\lambda}{\cosh\alpha\lambda}\right)^{\nu} B_3 \tag{26}$$

in which G represents the function

$$G \equiv \frac{\cosh\alpha - \left(\frac{\sinh\alpha\lambda}{\cosh\alpha\lambda}\right)^{\nu}\sinh\alpha}{\sinh\alpha - \left(\frac{\sinh\alpha\lambda}{\cosh\alpha\lambda}\right)^{\nu}\cosh\alpha} \tag{27}$$

In these equations, $\nu = 1$ for the conducting bottom wall, for which Equation (9a) applies, and $\nu = -1$ for the insulating bottom wall, for which Equation (9b) applies. The Marangoni number corresponding to neutral stability then follows from Equation (11)

$$M = \frac{2A_2}{\alpha B_2} \tag{28}$$

The solution is now complete. All of the constants are proportional to A_1; thus the value of A_1 does not affect the result and can be conveniently chosen to be 1. For specified values of $\mathcal{R}$, $\mathcal{A}$, $\mathcal{S}$, and λ, these equations determine M as a function of α, referred to as the curve of neutral stability. The minimum in that curve corresponds to the critical Marangoni number. A digital computer program was written to compute the values of the critical Marangoni number presented in Figures 2 through 4. This required $\Psi'(1)$ in addition to the functions given. The function $\Psi'(\eta)$ is readily obtained by differentiating Equation (20) with respect to η.

SOLUTION FOR INFINITE LIQUID DEPTH

A limiting case of considerable importance is that in which the liquid layer depth is much greater than the thickness of the concentration boundary layer, that is for λ

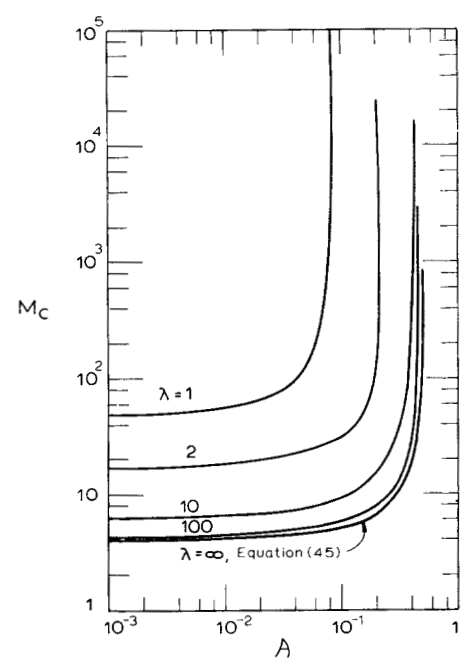

Fig. 4. Effect of liquid depth on M_c for conducting case, $\mathcal{R} = 0$, $\mathcal{S} = 0$.

approaching infinity. For this case, Equations (7) and (8) require that $f(\eta)$ and its first derivative must vanish as η approaches infinity. Taking p to be zero, the solution to Equation (4) which satisfies this condition and also satisfies Equation (10) is

$$f(\eta) = A_4 \eta e^{-\alpha\eta} \tag{29}$$

Adopting the definition

$$Q(\eta) \equiv f(\eta)\, \Phi'(\eta) \tag{30}$$

and taking p to be zero, Equation (5) becomes

$$(D^2 - \alpha^2) g = Q(\eta) \tag{31}$$

A general solution to this equation can be expressed in the form

$$g(\eta) = B_5 \sinh \alpha\eta + B_6 \cosh \alpha\eta - \frac{e^{-\alpha\eta}}{2\alpha} \int_a^\eta Q(u)\, e^{\alpha u}\, du + \frac{e^{\alpha\eta}}{2\alpha} \int_b^\eta Q(u)\, e^{-\alpha u}\, du \tag{32}$$

in which u is a dummy variable of integration and a, b, B_5, and B_6 are arbitrary constants. In order that Equation (9a) or Equation (9b) might be satisfied as λ approaches infinity, it is necessary that $B_6 = -B_5$ and also that $b = \infty$. Equation (32) then becomes

$$g(\eta) = B_5(\sinh \alpha\eta - \cosh \alpha\eta) - \frac{e^{-\alpha\eta}}{2\alpha} \int_a^\eta Q(u) e^{\alpha u}\, du - \frac{e^{\alpha\eta}}{2\alpha} \int_\eta^\infty Q(u)\, e^{-\alpha u}\, du \tag{33}$$

From this equation the following relationship is readily derived

$$g'(0) + \alpha g(0) = -\int_0^\infty Q(u)\, e^{-\alpha u}\, du \equiv I \tag{34}$$

Employing Equations (11) and (12), the grouping on the left-hand side of Equation (34) can be related to the Marangoni number

$$g'(0) + \alpha g(0) = I = (\mathcal{R} + \alpha^2 \mathcal{S} + \alpha) \left[\frac{f''(0)}{M\alpha^2} \right] - \mathcal{A} f'(0) \tag{35}$$

Rearranging yields

$$M = \frac{(\mathcal{R} + \alpha^2 \mathcal{S} + \alpha) f''(0)}{[1 + \mathcal{A} f'(0)]\alpha^2} \tag{36}$$

Using Equation (29), this equation becomes

$$M = \frac{-2\alpha A_4 (\mathcal{R} + \alpha^2 \mathcal{S} + \alpha)}{\alpha^2 (I + \mathcal{A} A_4)} \tag{37}$$

and the integral I is given by

$$I = -A_4 \int_0^\infty u\, \Phi'(u)\, e^{-2\alpha u}\, du \tag{38}$$

It is apparent from Equations (37) and (38) that the value of the constant A_4 has no effect upon the result and can therefore be conveniently chosen to be -1; Equations (37) and (38) then become

$$M = \frac{2\left(\frac{\mathcal{R}}{\alpha} + \alpha\mathcal{S} + 1\right)}{I - \mathcal{A}} \tag{39}$$

$$I = \int_0^\infty u e^{-2\alpha u}\, \Phi'(u)\, du = \frac{1}{h(C_B - C_i)} \int_{C_i}^{C_B} z e^{-2\alpha z/h}\, dC \tag{40}$$

The second equality in Equation (40) follows from the definitions of Φ and η; it is understood in the second integral that the relationship between z and C is that corresponding to the unperturbed concentration profile.

For any concentration profile in the unperturbed state, I can be evaluated by use of Equation (40), and Equation (39) then yields the curve of neutral stability.

General Solution for $\mathcal{R} = 0$

Of particular interest is the case in which the mass transfer is gas-phase controlled, that is the limit in which $\mathcal{R} = 0$. In this case, the neutral stability curve has the minimum value of M at $\alpha = 0$. This is apparent from Equations (39) and (40) because I is greatest at that point. Taking $\alpha = 0$, Equations (39) and (40) become

$$M_c = \frac{2}{I - A} \tag{41}$$

$$I = \frac{1}{h(C_B - C_i)} \int_{C_i}^{C_B} z\, dC = \frac{1}{h(C_B - C_i)} \int_0^\infty (C_B - C)\, dz \tag{42}$$

It is seen that the integrals in Equation (42) are equal to the solute deficiency in the liquid phase concentration boundary layer, corresponding to the shaded area in Figure 1c. This result applies to any unperturbed concentration profile, provided of course that C approaches C_B sufficiently rapidly at large values of z so that the integrals in Equation (42) will converge.

Until now the quantitative definition of h, the characteristic thickness of the concentration boundary layer in the liquid phase, has been left unspecified except for the case of the broken line profile of Figure 1b. Equation (42) suggests the general definition of h which will render the critical Marangoni number independent of the shape of the unperturbed concentration profile when $\mathcal{R} = 0$. The definition adopted for h is given by

$$\frac{1}{2} h\, (C_B - C_i) \equiv \int_{C_i}^{C_B} z\, dC = \int_0^\infty (C_B - C)\, dz \tag{43}$$

Therefore h is seen to be the thickness of a broken line profile with the same solute deficiency as the actual concentration profile in the unperturbed state, as shown in Figure 1d, in which the two shaded sections are of equal area. With this definition of h, Equation (42) yields

$$I = \frac{1}{2} \tag{44}$$

and Equation (41) becomes

$$M_c = \frac{2}{\frac{1}{2} - \mathcal{A}} \tag{45}$$

This result is general, independent of the shape of the unperturbed concentration profile, when $\mathcal{R} = 0$. It shows that the critical value of $\mathcal{A}$ is 0.5; at this value, surface convection in the Gibbs layer completely stabilizes the system, raising the critical Marangoni number to infinity.

Solution for $\mathcal{R} > 0$

When $\mathcal{R}$ is greater than zero, the minimum in the curve of M versus α will generally not occur at $\alpha = 0$, and M_c will not be independent of the shape of the unperturbed concentration profile. Nevertheless, Equation (43) will be

maintained as the definition of h. With this choice, $I = 0.5$ when $\alpha = 0$, and I decreases with increasing α, as is apparent from Equation (40). Therefore, as $\mathcal{A}$ approaches 0.5, the critical value of α decreases toward zero and the critical Marangoni number approaches infinity. Thus the critical value of $\mathcal{A}$ is equal to 0.5; this corresponds to an inventory in the Gibbs layer exactly equal to the solute deficiency in the liquid phase, as is apparent from the definitions of $\mathcal{A}$ and h. It is interesting to note that at this point surface convection completely stabilizes the system, irrespective of the value of $\mathcal{R}$ and irrespective of the shape of the unperturbed concentration profile.

For values of $\mathcal{A}$ less than 0.5 and for values of $\mathcal{R}$ greater than zero, M_c will depend upon the shape of the unperturbed concentration profile. Perhaps the simplest profile which might be investigated is the broken line profile given by Equation (13) and shown in Figure 1b. For this profile, Equation (40) yields

$$I = \int_0^1 ue^{-2\alpha u}\,du = \left[\frac{1}{4\alpha^2}\right]\left[1 - e^{-2\alpha}(1 + 2\alpha)\right] \quad (46)$$

and the curve of neutral stability becomes

$$M = \frac{2\left(\dfrac{\mathcal{R}}{\alpha} + \alpha\mathcal{S} + 1\right)}{\left[\dfrac{1}{4\alpha^2}\right]\left[1 - e^{-2\alpha}(1 + 2\alpha)\right] - \mathcal{A}} \quad (47)$$

The minimum in this curve corresponds to the critical Marangoni number. Equation (47) was used to compute the solid curves in Figure 5, except for the bottom curve for $\mathcal{R} = 0$ which was computed from Equation (45).

In order to determine the effect of differing shapes of the unperturbed concentration profile, it is useful to compare the results for the broken line profile with those obtained from the profile corresponding to a liquid phase penetration theory with a constant gas phase mass transfer coefficient, as given by Crank (1956):

$$\frac{C_B - C}{C_B - C^*} = \operatorname{erfc}\left[\frac{z}{2\sqrt{\mathcal{D}\theta}}\right] - \exp\left[\frac{Hk_G z}{\mathcal{D}} + \frac{(Hk_G)^2\theta}{\mathcal{D}}\right]\operatorname{erfc}\left[\frac{z}{2\sqrt{\mathcal{D}\theta}} + \frac{Hk_G\sqrt{\theta}}{\sqrt{\mathcal{D}}}\right] \quad (48)$$

In this equation θ represents the penetration theory contact time, and C^* is the liquid phase solute concentration in equilibrium with the bulk gas phase partial pressure. For this profile, Equation (43) yields the result

$$h = \frac{4\sqrt{\dfrac{\mathcal{D}\theta}{\pi}}}{1 - \exp\left[\dfrac{(Hk_G)^2\theta}{\mathcal{D}}\right]\operatorname{erfc}\left[\dfrac{Hk_G\sqrt{\theta}}{\sqrt{\mathcal{D}}}\right]} - \frac{2\mathcal{D}}{Hk_G} \quad (49)$$

Employing Equations (48) and (49) to characterize the unperturbed concentration profile, Equations (40) and (39) can be used to compute the curve of neutral stability and thus the critical Marangoni number. The results obtained (Ross, 1972), using numerical evaluation of the integral in Equation (40), are shown as the dashed curves in Figure 5.

DISCUSSION OF RESULTS

As in the paper by Brian (1971), it is found here that surface diffusion in the Gibbs layer has a negligible effect on M_c. Therefore it will not be considered further, and all the results to be presented are for $\mathcal{S} = 0$.

Figure 2 shows the effects of $\mathcal{A}$ and $\mathcal{R}$ on the critical Marangoni number for the case of an insulating bottom wall with $\lambda = 10$. It is seen that M_c increases with increasing $\mathcal{R}$ and with increasing $\mathcal{A}$, and indeed M_c approaches infinity as $\mathcal{A}$ approaches a critical value which is independent of $\mathcal{R}$. Figures 3 and 4 show the effect of λ for the insulating and conducting cases, respectively, for gas phase controlled mass transfer $\mathcal{R} = 0$. For $\lambda = 1$, these results correspond to those presented by Brian (1971). Increasing values of λ represent increasingly deep liquid layers, relative to the mass transfer penetration depth. At large values of λ, the results for the insulating and conducting cases approach each other, in agreement with the obvious requirement that conditions at the bottom wall lose significance when the liquid is very deep. The lowest curves in Figures 3 and 4 are for $\lambda = \infty$, as given by Equation (45).

The effect of the shape of the unperturbed concentration profile has been investigated only for the case of an infinitely deep liquid layer. Figure 5 compares results for the penetration theory profile Equation (48) with those for the broken line profile. When $\mathcal{R} = 0$, the curves are identical and are given by Equation (45). With $\mathcal{R} > 0$, the curves differ but little, indicating the very low sensitivity of the result to the shape of the unperturbed concentration profile.

APPLICATION TO PENETRATION MASS TRANSFER

In penetration-type mass transfer, the penetration depth h and the solute deficiency increase with contact time; thus M will increase and $\mathcal{A}$ will decrease. The onset of instability will occur when M exceeds the value of M_c corresponding to the instantaneous values of $\mathcal{R}$, $\mathcal{A}$, and λ.

The application of the present results to the prediction of the onset of instability will be illustrated by the example of triethylamine desorption from water, as in the short

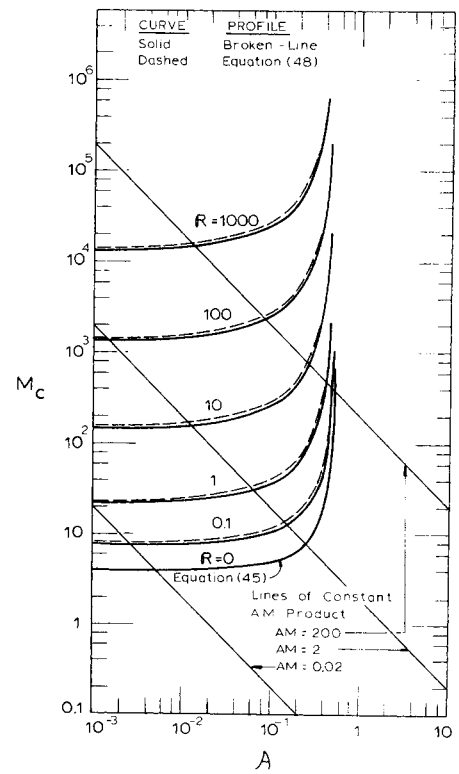

Fig. 5. Critical Marangoni number for infinite liquid depth, $\mathcal{S} = 0$.

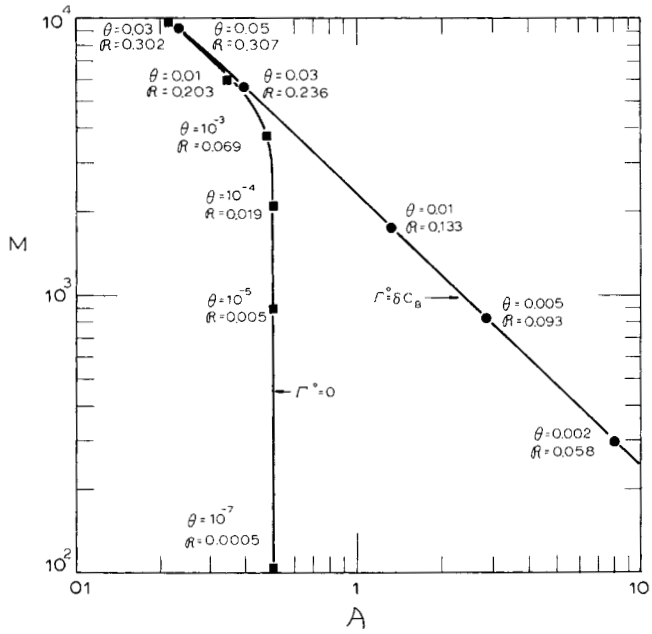

Fig. 6. Experimental paths for triethylamine desorption.

TABLE 1. TRIETHYLAMINE DESORPTION FROM WATER AT 298°K

$\sigma = 1.23 \times 10^6$ (dyne)(cm²)/g-mole	$\mathcal{D}$ =	0.82×10^{-5} cm²/s
$\delta = 0.496 \times 10^{-4}$ cm	Hk_G =	2.21×10^{-3} cm/s
$\mu = 0.894 \times 10^{-2}$ (dyne)(s)/cm²	C_B =	3×10^{-6} g-moles/cm³
	C^* =	0

wetted-wall column experiments of Brian et al. (1971). The physical parameters employed in this example are listed in Table 1; they are given in the above named reference and also in more detail by Mayr (1970).

Gibbs Effect on Unperturbed Profile

Equation (48) represents the unperturbed concentration profile for a penetration theory model of the liquid phase with a constant gas phase resistance, but neglecting solute storage in the Gibbs adsorption layer. When storage in the Gibbs layer is included in the analysis, assuming δ to be constant, the result (Ross, 1972) is

$$Y \equiv \frac{C_B - C}{C_B - C^*} = \operatorname{erfc}\left[\frac{z}{2\sqrt{\mathcal{D}\theta}}\right] + \left[\frac{L/J + Y_i^0 J}{J - F}\right] \exp\left[\frac{Jz}{\delta} + \frac{J^2\mathcal{D}\theta}{\delta^2}\right] \operatorname{erfc}\left[\frac{z}{2\sqrt{\mathcal{D}\theta}} + \frac{J\sqrt{\mathcal{D}\theta}}{\delta}\right] - \left[\frac{L/F + Y_i^0 F}{J - F}\right] \exp\left[\frac{Fz}{\delta} + \frac{F^2\mathcal{D}\theta}{\delta^2}\right] \operatorname{erfc}\left[\frac{z}{2\sqrt{\mathcal{D}\theta}} + \frac{F\sqrt{\mathcal{D}\theta}}{\delta}\right] \quad (50)$$

This equation involves an important new parameter

$$Y_i^0 \equiv \frac{C_B - \Gamma^0/\delta}{C_B - C^*} \quad (51)$$

in which Γ^0 represents the inventory in the Gibbs adsorption layer at the beginning of the penetration theory contact interval. Employing Equation (43) it can be shown that, for this profile, h is given by

$$Y_i h = 2\sqrt{\frac{\mathcal{D}\theta}{\pi}} - \frac{\mathcal{D}}{Hk_G} - \delta\left[\frac{L/J^2 + Y_i^0}{J - F}\right] \exp\left[\frac{J^2\mathcal{D}\theta}{\delta^2}\right] \operatorname{erfc}\left[\frac{J\sqrt{\mathcal{D}\theta}}{\delta}\right] + \delta\left[\frac{L/F^2 + Y_i^0}{J - F}\right] \exp\left[\frac{F^2\mathcal{D}\theta}{\delta^2}\right] \operatorname{erfc}\left[\frac{F\sqrt{\mathcal{D}\theta}}{\delta}\right] \quad (52)$$

in which Y_i is obtained by substituting $z = 0$ into the right-hand side of Equation (50).

Consider two experimental cases. In one case $\Gamma^0 = 0$, which corresponds to an absence of solute in the Gibbs layer at the beginning of the contact interval. This might be thought to approximate the entrance conditions in short wetted-wall column experiments in which the liquid surface has been freshly formed at $\theta = 0$. In the other case $\Gamma^0 = \delta C_B$ which corresponds to the Gibbs layer being in equilibrium with the bulk liquid concentration at the start of the contact interval. This might represent an experiment in which a liquid phase was equilibrated with a gas phase containing triethylamine, and then at $\theta = 0$ the gas phase was suddenly replaced by fresh gas containing no triethylamine.

Figure 6 shows the experimental paths calculated using Equation (50) for these two limiting cases, as represented in a graph of M versus $\mathcal{A}$. When $\Gamma^0 = \delta C_B$, Γ varies but little with θ. Therefore as $h(C_B - C_i)$ increases with increasing θ, M increases and $\mathcal{A}$ decreases but the product of M and $\mathcal{A}$

$$\mathcal{A}M = \frac{\sigma\Gamma}{\mu\mathcal{D}} = \frac{\sigma\delta C_i}{\mu\mathcal{D}} = \frac{\sigma^2 C_i}{\mu\mathcal{D}RT} \quad (53)$$

remains approximately constant, and the experimental path

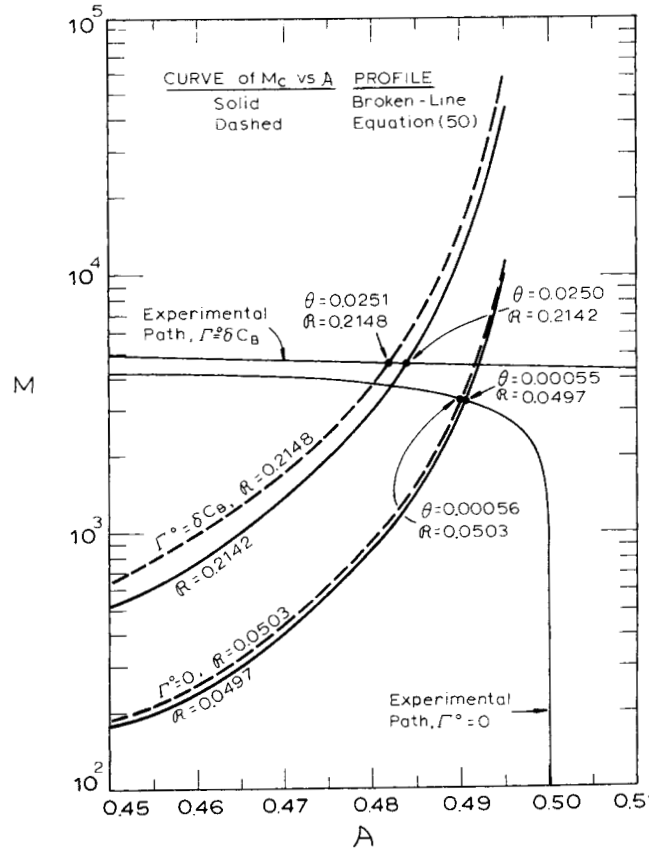

Fig. 7. Onset of instability for infinite liquid depth.

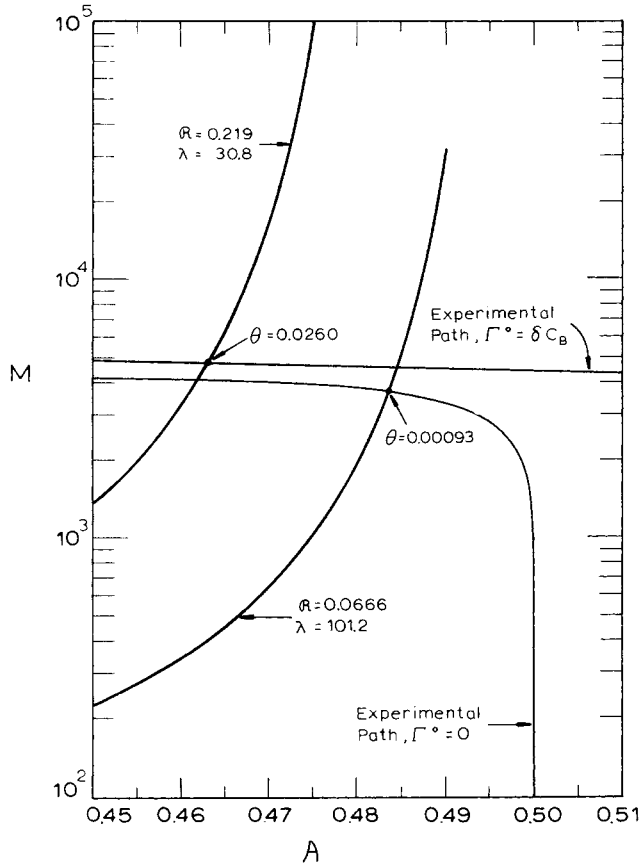

Fig. 8. Onset of instability for finite depth, insulating case, $l = 0.025$ cm, $S = 0$.

in Figure 6 approximates a straight line of slope -1. In contrast, when Γ^0 and C^* are both zero, the initial solute transfer is largely from the liquid phase to the Gibbs layer, with little transfer to the gas phase. Thus Γ approximately equals the solute deficiency, and $\mathcal{A}$ remains nearly 0.5 as M increases. Later, as solute transfer to the gas phase becomes appreciable, $\mathcal{A}$ will decrease. At long times, the experimental paths for these two cases approach each other as shown in Figure 6.

When a path in Figure 6 intersects the appropriate curve of M_c versus $\mathcal{A}$, the point of instability is reached. For the case of an infinite liquid depth, these intersections are shown in Figure 7. The two experimental paths are the same as those shown in Figure 6. The solid curves of M_c versus $\mathcal{A}$ were obtained using the broken line unperturbed concentration profile and choosing the values of $\mathcal{R}$ which correspond to the experimental paths at the points of intersection. The dashed curves of M_c versus $\mathcal{A}$ were obtained using the profiles actually prevailing in the experimental paths at the points of intersection, as given by Equation (50) with the physical parameters for triethylamine. It is seen again that the result is insensitive to the choice of unperturbed profile.

Figure 8 shows the intersection points when the liquid depth is 0.025 cm, as in the experiments of Brian et al. (1971). The experimental paths are the same as those in Figures 6 and 7, based on Equation (50); this should be an adequate approximation even for this finite liquid depth. The curves of M_c versus $\mathcal{A}$ have been obtained employing the broken line profile. In view of the insensivity of M_c to profile shape, seen in Figures 5 and 7, this should also be a suitable approximation.

It is seen in Figures 7 and 8 that the result for $l = 0.025$ cm is close to that for $l = \infty$. On the other hand, Γ^0 has a major effect. The contact times at the onset of instability for the two values of Γ^0 are seen to differ by factors of 28 and 45. This sensitivity to Γ^0 will introduce considerable uncertainty in predicting the point of instability in many experimental situations. For example, when liquid mixing occurs periodically, as in a packed tower, each mixing may not completely destroy the Gibbs layer and the value of Γ^0 will be obscure.

Effect of Surface Convection in the Gibbs Layer

For either experimental path, surface convection in the Gibbs layer has a profound effect on the predicted point of inception of instability. Neglecting surface convection, the curves of M_c versus $\mathcal{A}$ for these cases would be horizontal lines at $M_c \cong 4$, which would intersect the experimental paths at $\theta = 6 \times 10^{-5}$ s for $\Gamma^0 = \delta C_B$ and $\theta = 2 \times 10^{-10}$ s for $\Gamma^0 = 0$. These values of θ are lower than the ones shown in Figures 7 and 8 by factors of 400 and several million for the respective values of Γ^0.

Without surface convection, the critical Marangoni number would be equal to 4; with surface convection in the Gibbs layer, the critical Marangoni number is approximately 4,000 for the cases shown in Figures 7 and 8. This thousand-fold increase in M_c results from the strong surface activity of triethylamine, as measured by its $\mathcal{A}M$ product of 2,200.

Consider cases with $\Gamma^0 = \delta C_B$, for which the $\mathcal{A}M$ product varies little with θ. When the solute is very weakly surface active, the $\mathcal{A}M$ product will be small, and the experimental path will be similar to the line for $\mathcal{A}M = 0.02$ shown in Figure 5. Assuming $\mathcal{R} \cong 0$, this path will intersect the curve of M_c versus $\mathcal{A}$ at $M \cong 4$, the result obtained without surface convection in the Gibbs layer. On the other hand, when the solute is strongly surface active, for example with $\mathcal{A}M = 200$, instability occurs essentially when $\mathcal{A}$ falls below 0.5, and the critical value of $\mathcal{A}$ is more significant than the critical Marangoni number. When $\mathcal{R} \cong 0$, the line for $\mathcal{A}M = 2$ is seen in Figure 5 to divide the region in which surface convection is negligible from that in which surface convection is dominant.

Comparison with Experiment

The value $C_B = 3 \times 10^{-6}$ g.-moles/cm^3 employed in this example calculation is approximately the value found experimentally (Brian et al., 1971) to correspond to the inception of Marangoni convection in short wetted-wall column experiments with a contact time of 0.17 seconds. At $\theta = 0.17$ the value of M for both experimental paths shown in Figure 6 corresponds approximately to 30,000. This is 8 times the values of M_c predicted by the intersections in Figures 7 and 8, but it is 8,000 times the value $M_c = 4$ predicted in the absence of surface convection in the Gibbs adsorption layer.

CONCLUDING REMARKS

The eight thousand-fold discrepancy between the experimentally measured and the predicted values of the critical Marangoni number for triethylamine desorption has been reduced to an eight-fold discrepancy by incorporating into the hydrodynamic stability theory the effect of surface convection in the Gibbs adsorption layer. The residual eight-fold discrepancy may result from inadequacies in the present theory due to the use of the frozen-profile assumption. On the other hand, it is also possible that other differences between the present theory and the experimental system might have caused the discrepancy. The presence of nonvolatile surface active contaminants in the experimental system would have raised the observed critical Marangoni number (Berg and Acrivos, 1965). Another possibility is the effect of the inlet and outlet liq-

uid slots in the short wetted-wall column experiment, which probably represent a stabilizing influence not present in the theoretical model, which treats a liquid of infinite expanse in the surface coordinate directions.

The other solutes studied by Brian et al. (1971) are not as strongly surface active as triethylamine. For these solutes, the experimental values of M_c show smaller deviations from the earlier theory which neglected Gibbs adsorption, but the increase in M_c due to the effect of Gibbs adsorption is also smaller, leaving a residual discrepancy as in the case of triethylamine. It is beyond the scope of this paper to present a complete analysis of the experimental results on the critical Marangoni number. The resolution of the residual discrepancy will probably require additional research along both theoretical and experimental lines. But the thousand-fold increase in the critical Marangoni number due to surface convection in the Gibbs adsorption layer is a profound effect which must surely be included in any theoretical model of Marangoni instability for the desorption of triethylamine and other strongly surface active solutes.

ACKNOWLEDGMENT

Financial support from the National Science Foundation is gratefully acknowledged.

NOTATION

$A_1, A_2 \ldots$ = arbitrary constants in Equations (14) and (29)
$\mathcal{A}$ = $\Gamma/h(C_B - C_i)$, the adsorption number; represents surface convection in the Gibbs layer
a = arbitrary constant in Equation (32)
$B_1, B_2 \ldots$ = arbitrary constants in Equations (18), (19), and (32)
b = arbitrary constant in Equation (32)
C = unperturbed solute concentration in liquid phase, g-moles/cm^3
C^* = value of C in equilibrium with bulk gas, g-moles/cm^3
c = perturbation in C, g-moles/cm^3
D = $d/d\eta$
$\mathcal{D}$ = diffusion coefficient for solute in liquid phase, cm^2/s
$\mathcal{D}_s$ = surface diffusion coefficient for solute, cm^2/s
$F(\xi, \zeta)$ = function representing variation of w and c with x and y
$F = \dfrac{1 + \sqrt{1 - 4L}}{2}$
$f(\eta)$ = function representing the variation of w with z
G = function defined by Equation (27)
$\mathcal{G}$ = δ/h, represents accumulation in the Gibbs layer
$g(\eta)$ = function which represents the variation of c with z
H = Henry's law constant for solute, (atm)(cm^3)/g-mole
h = mass transfer penetration depth, or concentration boundary layer thickness, in liquid phase, cm; defined by Equation (43)
I = integral defined in Equation (34)
$J = \dfrac{1 - \sqrt{1 - 4L}}{2}$
k_G = gas-phase mass transfer coefficient, g-moles/(s)(cm^2)(atm)
L = $Hk_G\delta/\mathcal{D}$
l = depth of liquid layer, cm
$M = \dfrac{\sigma(C_B - C_i)h}{\mu\mathcal{D}}$, the Marangoni number
p = growth rate constant for the disturbances, Equations (1) and (2)
$Q(\eta)$ = $f(\eta)\,\Phi'(\eta)$
$\mathcal{R}$ = $Hk_Gh/\mathcal{D}$, liquid-to-gas-phase resistance ratio
R = ideal gas law constant, 8.314×10^7 erg/g-mole)(°K)
$\mathcal{S}$ = $\mathcal{D}_s\delta/\mathcal{D}h$; represents surface diffusion in the Gibbs layer
Sc = Schmidt number for solute in liquid phase
T = absolute temperature, °K
t = time of growth or decay of a perturbation
u = dummy variable in definite integral
w = velocity in the z direction, cm/s
Y = defined by Equation (50)
x, y = position coordinates in the horizontal plane, cm
z = coordinate in the vertical direction, measured downward from the gas-liquid interface, cm

Greek Letters

α = wave number for periodic variation of $F(\xi, \zeta)$
Γ = surface concentration of solute in Gibbs adsorption layer in the unperturbed state, g-moles/cm^2
δ = Γ/C_i, the Gibbs depth; $\delta = \sigma/RT$ according to the Gibbs adsorption isotherm, cm
ζ = y/h
η = z/h
θ = contact time in penetration theory, s
λ = l/h
μ = liquid viscosity, (dyne)(s)/cm^2
ν = exponent in Equations (25), (26), and (27); $\nu = 1$ for conducting case, and $\nu = -1$ for insulating case
ξ = x/h
σ = negative of the slope of the curve of surface tension versus solute concentration, evaluated at C_i, (dyne)(cm^2)/g-mole
τ = $t\mathcal{D}/h^2$
$\Phi(\eta)$ = function defined by Equation (6)
$\Psi(\eta)$ = function defined by Equation (20)

Subscripts and Superscripts

B = bulk liquid
c = critical value
i = gas-liquid interface
^{0} = value at $\theta = 0$
$'$ = differentiation with respect to η

LITERATURE CITED

Adamson, A. W., "Physical Chemistry of Surfaces," 2nd. ed., pp. 80-81, Interscience, New York (1967).

Berg, J. C., and A. Acrivos, "The Effect of Surface Active Agents on Convection Cells Induced by Surface Tension," *Chem. Eng. Sci.*, **20**, 737 (1965).

Blair, L. M., and J. A. Quinn, "The Onset of Cellular Convection in a Fluid Layer with Time-Dependent Density Gradients," *J. Fluid Mech.*, **36**, 385 (1969).

Brian, P.L.T., "Effect of Gibbs Adsorption on Marangoni Instability," *AIChE J.*, **17**, 765 (1971).

———., J. E. Vivian, and S. T. Mayr, "Cellular Convection in Desorbing Surface Tension-Lowering Solutes from Water," *Ind. Eng. Chem. Fundamentals*, **10**, 75 (1971).

Brian, P. L. T., and K. A. Smith, "Influence of Gibbs Adsorption on Oscillatory Marangoni Instability," *AIChE J.*, **18**, 231 (1972).

Crank, J., "The Mathematics of Diffusion," p. 34, Oxford Univ. Press, London, England (1956).

Deardorff, J. W., "Gravitational Instability between Horizontal Plates with Shear," *Phys. Fluids*, **8**, 1027 (1965).

Foster, T. D., "Stability of a Homogeneous Fluid Cooled Uniformly from Above," *Ibid.*, 1249 (1965a).

———., "Onset of Convection in a Layer of Fluid Cooled from Above," *ibid.*, 1770 (1965b).

———., "Effect of Boundary Conditions on the Onset of Convection," *ibid.*, **11**, 1257 (1968).
Gallagher, A. P., and A. McD. Mercer, "On the Behaviour of Small Disturbances in Plane Couette Flow with a Temperature Gradient," *Proc. Roy. Soc. (London), A286*, 117 (1965).
Gresho, P. M., and R. L. Sani, "The Stability of a Fluid Layer Subjected to a Step Change in Temperature: Transient vs. Frozen Time Analysis, *Intern J. Heat Mass Transfer*, **14**, 207 (1971).
Mahler, E. G., R. S. Schechter, and E. H. Wissler, "Stability of a Fluid with Time-Dependent Density Gradients," *Phys. Fluids*, **11**, 1901 (1968).
Mayr, S. T., "Mass Transfer Enhancement in Gas-Liquid Systems due to the Marangoni Effect," Sc.D. thesis, Mass. Inst. Technol., Cambridge (1970).
Pearson, J. R. A., "On Convection Cells Induced by Surface Tension," *J. Fluid Mech.*, **4**, 489 (1958).
Ross, J. R., "The Effect of Gibbs Adsorption on Marangoni Instability," Ph.D. thesis, Mass. Inst. Technol., Cambridge (in preparation, 1972).
Scriven, L. E., and C. V. Sternling, "On Cellular Convection Driven By Surface Tension Gradients: Effects of Mean Surface Tension and Surface Viscosity," *J. Fluid Mech.*, **19**, 321 (1964).
Smith, K. A., "On Convective Instability Induced by Surface-Tension Gradients," *J. Fluid Mech.*, **24**, 401 (1966).
Spangenberg, W. G., and W. R. Rowland, "Convective Circulation in Water Induced by Evaporative Cooling," *Phys. Fluids*, **4**, 743 (1961).
Vidal, A., and A. Acrivos, "Effect of Nonlinear Temperature Profiles on the Onset of Convection Driven by Surface Tension Gradients," *Ind. Eng. Chem. Fundamentals*, **7**, 53 (1968).

Manuscript received December 9, 1971; revision received February 9, 1972; paper accepted February 9, 1972.

The Interrelationship Between Bubble Motion and Solids Mixing in a Gas Fluidized Bed

A. K. HAINES and R. P. KING

National Institute for Metallurgy Research Group, University of Natal, Durban, South Africa

E. T. WOODBURN

Department of Chemical Engineering, University of Natal, Durban, South Africa

The stochastic differential equations for particle motion in a homogeneous fluidized bed have been modified to incorporate a bubble-particle interaction. In a freely bubbling bed this interaction causes an instantaneous random step upwards when a particle collides with a bubble. In addition the particles are subject to a Brownian Motion due to particle-particle interactions and to a vertical drift velocity. The particle motion was modeled by the set of stochastic differential equations

$$dU = -U + dW$$
$$dX = (U_x + \bar{U})\,dt + S\,dN$$
$$dY = U_y dt$$
$$dZ = U_z dt$$

where N and W are Poisson and Wiener processes respectively. U is the velocity vector, X the vertical coordinate, Y and Z the horizontal coordinates. This set of equations has been solved and the form of the probability density function $p(x, t)$ has been obtained. Predictions are in terms of the mean bubble frequency at a point λ the average displacement associated with a particle-bubble collision, and the dense phase diffusion coefficient.

The main result is that the effective diffusion coefficient in the vertical direction is given by

$$E^* = E + \lambda/\alpha^2$$

where E is the dense phase diffusion coefficient and $1/\alpha$ is the average displacement suffered by a particle on collision with bubble.

The model was tested experimentally using random forcing function techniques. All parameters were evaluated independently; λ by direct measurement and the other two inferred from available published data. The predictions of the theory agreed well with experimental observations of the solids dispersion.

The effects of solids mixing on temperature control, heat transfer, and chemical conversion in a gas fluidized bed are well known.

Since the pioneering work of Rowe and Partridge (*1*),